S-Parameter Characterization of mm-Wave IMPATT Oscillators

Jürgen Hasch[1], Erich Kasper[2]
[1]Robert Bosch GmbH, Central Research and Development, CR/ARE1
P.O. Box 10 60 50, 70049 Stuttgart, Germany
[2]Institut für Halbleitertechnik, Universität Stuttgart
Pfaffenwaldring 47, 70569 Stuttgart, Germany

Abstract — **Designing oscillators in a fully monolithically integrated technology requires accurate characterization of the active element, as well as the surrounding passive circuitry. Based upon S parameter measurements of Impatt diodes, millimeter wave oscillators up to 124 GHz have been designed,manufactured and measured. Two measurements setups covering the frequency range from 0.04 - 140 GHz were used and a careful calibration approach was applied.**

I. Introduction

One attractive approach for realizing cost-effective millimeter wave circuits is the monolithic integration of passive circuit elements along with semiconductor devices on high resistivity silicon (SIMMWIC Silicon monolithic mm-wave integrated circuits).

The high permittivity of silicon allows for small dimensions of passive circuitry with low losses due to the high resistivity silicon. Additionally, using advanced epitaxy, semiconducting devices can be integrated on silicon, directly integrated with the surrounding passive elements. Recently, our group succeeded to integrate monolithically IMPATT diodes into SIMMWIC circuits. Discrete IMPATT diodes were used for a long time in hybrid circuits. Monolithic integration was considered difficult because of low negative impedance levels and operation in the avalanche multiplication regime.

Low manufacturing costs can be achieved because of relaxed requirements for the photolithographic processing. A feature resolution in the order of 1 µm is sufficient to realize millimeter wave components above 100 GHz. Also, only a few mask steps are required, further reducing processing complexity. In this case, five mask steps are needed.

As complete monolithic integration practically eliminates all tuning capabilities after wafer processing, therefore an accurate characterization of the elements is required for circuit design.

In this paper we considered the principal requirements of S parameter measurements of devices with negative differential resistance. Based on device characterization, IMPATT oscillators in the millimeter waver frequency regime up to 124 GHz were designed, fabricated and tested.

II. S Parameter Measurement Setup

To characterize passive and active integrated components in the millimeter wave range, a Cascade Summit 12651B onwafer probe station with a HP 8510 or Anritsu ME 7808 network analyzer has been used. The HP 8510 was used together with a pair of OML V08VNA millimeter wave heads for measurements in the F waveguide band, covering the frequency range of 90-140 GHz. The Anritsu ME7808 network analyzer was used to cover the frequency range 0.04-110 GHz.

When measuring S parameters of active devices, in this case an Impatt diode, small signal operation of the device is usually assumed. Because the test port power coming from the network analyzer is much less than 1% of the DC biasing power applied to the Impatt diode, the diode is assumed to be operating in small signal operation. Figure 1 shows the output power at the network analyzer test port for the covered frequency range. The output power values below 65 GHz were not measured and taken from the instrument specifications.

For small bias currents of the Impatt diode, power leveling may be applied for the lower frequency range under 65 GHz. However, in this case, such biasing conditions are not relevant for the design of oscillators working above 100 GHz.

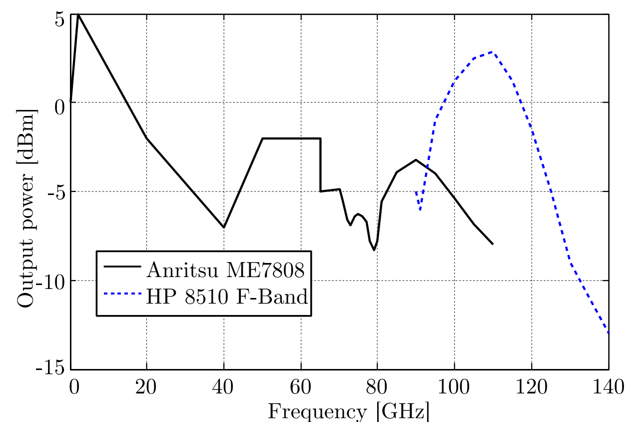

Fig. 1: Network analyzer test port output power

When making measurements with waveguide based equipment, care has to be taken when selecting the on-wafer prober head. Because the Impatt diode exhibits its active characteristics in a broad frequency band, parasitic oscillations may occur, if the prober head doesn't exhibit a proper match, even outside its working range. To achieve stable measurements, fulfilling the oscillation condition must be avoided over the complete frequency range, where the diode can act as an active component. Therefore, the onwafer prober head needs to provide a sufficient match to the diode.

Figure 2 shows the input reflection for three different waveguide prober heads, looking from the on-wafer side (integrated circuit side) into the prober head (measurement equipment side).

It can be noticed, that for this kind of measurements, the Cascade prober head should not be used. It exhibits a large

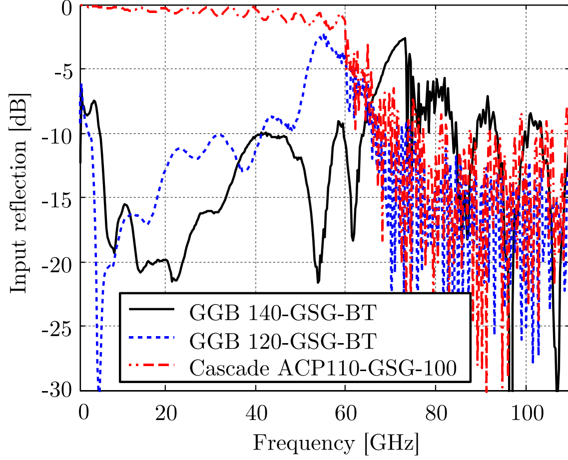

Fig. 2: Input reflection of different on-wafer prober heads

reflection below 60 GHz, which may lead to undesired oscillations. The tested prober heads from GGB show a more desirable behavior.

When contacting aluminum pads with an onwafer prober head, contact resistance and reproducibility problems will occur, because the aluminum surface will oxidize quickly. Nickel alloy contacts can improve the contacting performance significantly.

III. Calibration and Deembedding

For on-wafer S parameter measurements, a two step approach is taken. In the first step, a SOL calibration on precision calibration substrate is performed. As second step, an additional deembedding procedure [1] is applied, using open-end and short-circuit deembedding structures. Figure 3 shows the short and open elements used for deembedding the Impatt diodes.

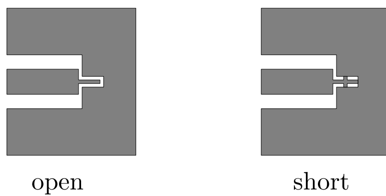

Fig. 3: Open-end and short-circuit deembedding elements.A short coplanar transmission line, allows placing the on-wafer prober head.

This approach has been taken, because calibration schemes with standards realized directly on-wafer have been found to be problematic. Contacting aluminum metallization with a prober head suffers from unreliable contacts. Novel contact materials like nickel alloy improve the situation for repetitive contacting, but do not mend the situation. Such contact problems typically lead to poor and unstable calibrations. This is especially true for modern network analyzers with limited hardware performance. These instruments rely on high quality calibrations.

After calibration, using an alumina calibration substrate with gold traces and precision loads, the short and open deembedding elements are measured.

In the given deembedding scheme, the S parameters have to be converted to admittances:

$$y = \frac{1 - S_{11}}{1 + S_{11}}$$

After measuring the device under test, the deembedding scheme can be applied by using the equation

$$z_{\text{deembedded}} = \frac{1}{y_{\text{meas}} - y_{\text{open}}} - \frac{1}{y_{\text{short}} - y_{\text{open}}}$$

and finally

$$S_{\text{deembedded}} = \frac{z_{\text{deembedded}} - 1}{z_{\text{deembedded}} + 1}$$

Figure 4 shows measured S_{11} parameters for the short and open deembedding circuits. The phase length in both circuits is coming from the short coplanar transmission line segment. The open element exhibits a declining magnitude with frequency, due to radiation into the silicon substrate.

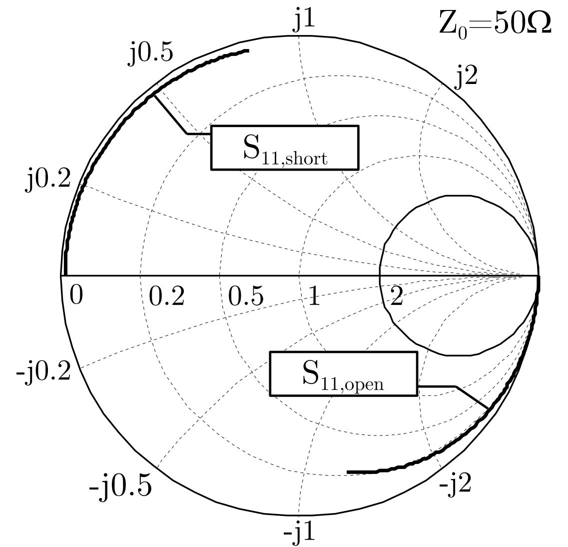

Fig. 4: Measured reflection coefficients for the short and open circuits in the frequency range 0-110 GHz.

In figure 5, the raw and deembedded Impatt diode S parameters for a 30x10 µm device are shown. The main difference between the curves is due to the reduced phase length, because the coplanar transmission line segment has been deembedded.

IV. Device Measurements

Figure 6 shows an Impatt diode, embedded in the measurement circuit. The Impatt diode can be seen as a long finger in the middle of the picture.

The semiconductor layer stacking of the diode is shown in figure 7. Directly above the high resistivity silicon substrate, a monocrystaline buffer layer is placed to achieve a defect free regular silicon crystal grid. On top of it, the p-doped *buried layer* is used to electrically contact the bottom side of the diode with the aluminum signal traces. The next layer is the sparsely n-doped combined drift and avalanche

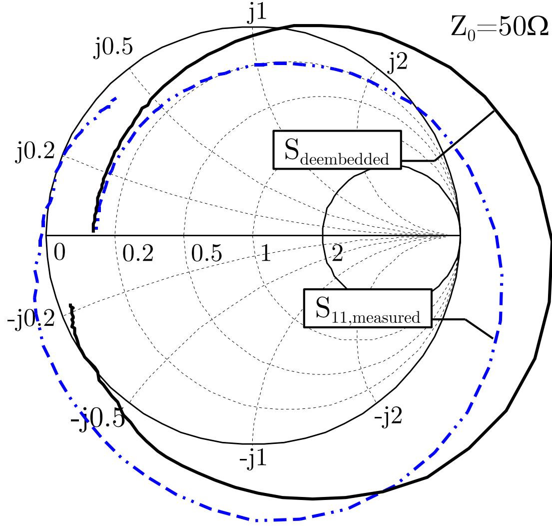

Fig. 5: Reflection coefficients before and after deembedding of a Impatt diode (diode area 30x10 µm,74 mA DC bias) in the frequency range 0-110 GHz.

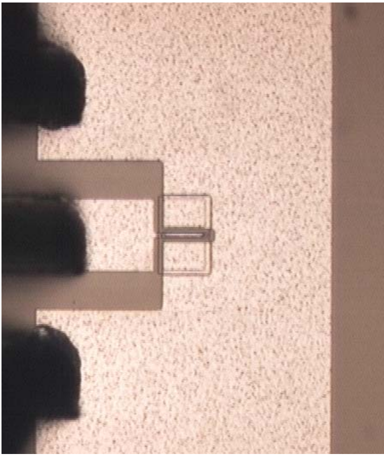

Fig. 6: Picture of a test circuit with the Impatt diode visible as a narrow finger in the middle. A on-wafer prober head connects the circuit from the left.

zone. On top of the semiconductor structure sits the highly doped n+ contact. The device properties are mainly controlled through the avalanche and drift zone thickness and the active device area. The growth of the layer stack by molecular beam epitaxy (MBE) and the processing by a low thermal budget process will be described elsewhere [2].

A number diodes with different lateral geometries have been manufactured and measured. The S parameter measurement results for a diode with an active area of 30x10 µm are shown in figure 8. Magnitude and phase of the S_{11} reflection parameter are shown for four different DC biasing conditions (50,60,70,80 mA) at a voltage of approximately 10 V. A broad peak of the magnitude around 60 GHz can be seen. When the magnitude exceeds one, the device exhibits active behavior. At its magnitude peak, the device has a zero phase crossing, which is usually referred to as avalanche frequency f_A. Above avalanche frequency, the reflection coefficient magnitude starts to decay and reaches unity at approximately one third above avalanche frequency.

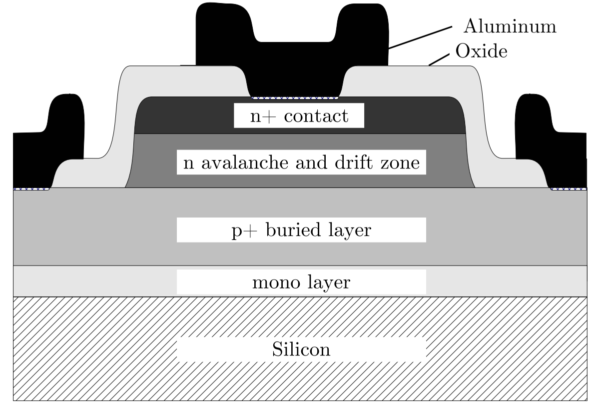

Fig. 7: Impatt diode layer stacking

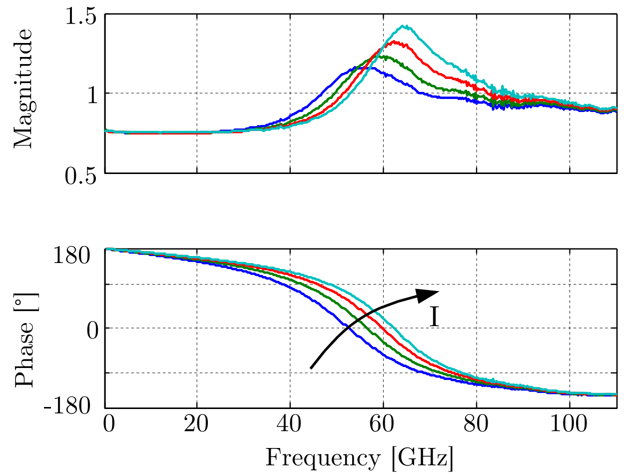

Fig. 8: S parameter magnitude and phase behavior of a 30x10 µm Impatt diode in the frequency range 0-110 GHz for biasing conditions 50,60,70,80 mA.

In figure 9, the measured avalanche frequency is shown as a function of the current density $J = I \cdot A$, where I is the biasing current and A is the active diode area. The expected theoretical behavior for the avalanche frequency from Read [3] is also shown in figure 9. The connection between avalanche frequency and current density given given by Read is

$$f_A \propto \sqrt{J}$$

It can be seen, that for increasing current densities, the avalanche frequency behavior will deviate from the theoretical curve. This is due to self-heating of the Impatt diodes for large current densities. The temperature behavior gets worse, as the diode area gets larger. At the end of the curve, the diode overheats and is destroyed.

The maximum reflection magnitude, measured at the avalanche frequency f_A, is shown in figure 10 for different Impatt diodes. The larger the active diode area, the larger the magnitude of the reflection coefficient gets.

V. Oscillator Design

As oscillator circuit, a simple shorted coplanar transmission line resonator has been used. This allow easy design and simple fabrication of the circuit, as no discontinuities or air bridges are necessary. Figure 11 shows the simpli-

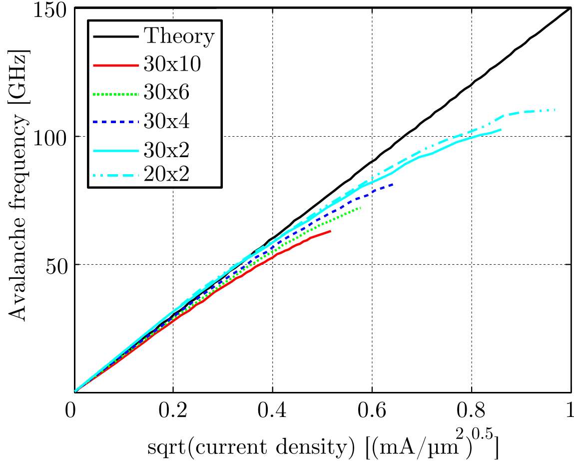

Fig. 9: Measured avalanche frequency of Impatt diodes with different active area sizes as a function of the square root of the current density.

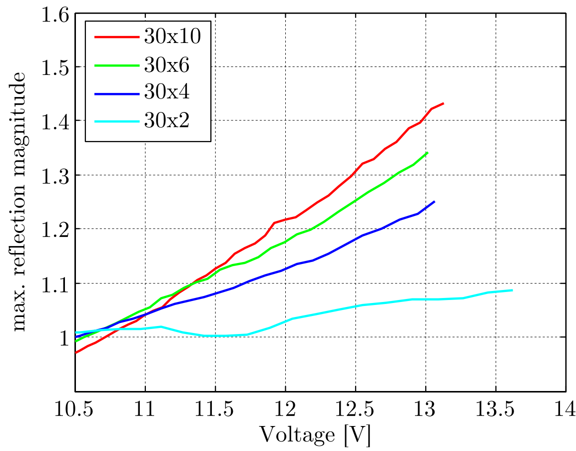

Fig. 10: Maximum reflection magnitude of an Impatt diode at avalanche frequency.

fied schematic diagram of the oscillator circuit. The circuit

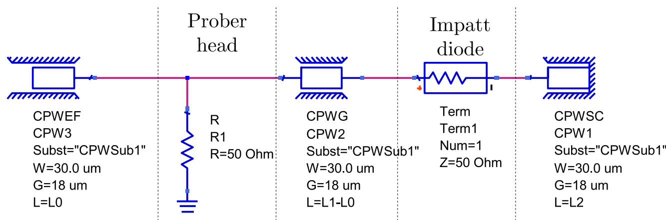

Fig. 11: Schematic of the Impatt oscillator with a short-circuited coplanar transmission line as resonator circuit.

is contacted at the open end transmission line with an on-wafer prober head. The contact position of the prober head can be freely selected, allowing a small degree of freedom in the exact impedance match between resonator circuit and Impatt diode. In conjunction with the Impatt diode, the resonant line length l_2 determines the oscillation frequency. The line length determines the phase of resonator circuit, while the shorted end results in a reflection coefficient magnitude of nearly one. The oscillating condition from [4] can be

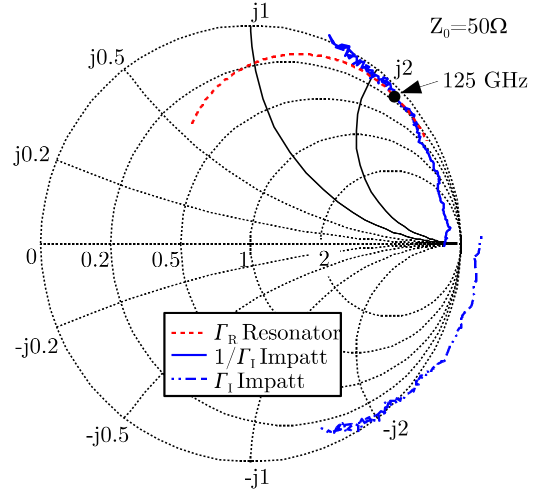

Fig. 12: Reflection coefficients of the coplanar resonator and the Impatt diode as a function of frequency. The frequency range is 90-140 GHz. The curves meet at approximately 125 GHz.

formulated in terms of reflection parameters as

$$\Gamma_\mathrm{R} = \frac{1}{\Gamma_\mathrm{I}}$$

Where Γ_R is the reflection coefficient of the coplanar resonator circuit presented to the Impatt diode and Γ_I is the reflection coefficient of the Impatt diode at a given DC biasing point.

The oscillating condition is met when the Γ_R and $\frac{1}{\Gamma_\mathrm{I}}$ curves cross each other at the same frequency. For the shown oscillator with $L_1 = 300\,\mu\mathrm{m}$ and $L_2 = 150\,\mu\mathrm{m}$, this is the case at about 125 GHz.

Figure 13 shows the layout of the designed oscillator circuit. The contact position of the on-wafer prober head, for measuring the oscillator output signal, is shown as outline. By moving the contact position, the magnitude of the resonator reflection coefficient Γ_R can be slightly adjusted.

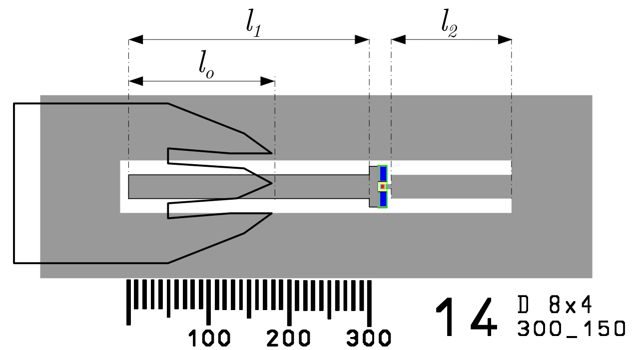

Fig. 13: Layout of an Impatt oscillator with a shorted coplanar line as resonator circuit. The onwafer prober head used for measuring the output spectrum is drawn as outline.

VI. Oscillator Measurements

The fabricated Impatt oscillators have been measured using a R&S FSEK30 spectrum analyzer with an external

waveguide mixer WHM-06 mixer from Farran [5]. To ensure a good match between the oscillator circuit and the mixer, an additional 10 dB attenuator is placed before the mixer. The conversion loss of the mixer is specified to be 40 dB at the oscillation frequency of 124.5 GHz, including the 10 dB attenuator losses.

Figure 15 shows the measured output spectrum of oscillator circuit for a DC operating point of 22 mA at 10.9 V. The measured oscillation frequency of 124.5 GHz agrees well with the expected value from the oscillator design. The prober head position was $L_0 = 220\,\mu\text{m}$.

The achieved power efficiency of the oscillator is quite low:

$$\eta = \frac{P_{\text{HF}}}{P_{\text{DC}}} = \frac{2\,\text{mW}}{240\,\text{mW}} \approx 0.8\%$$

Other realized oscillators with larger active areas of the diode exhibit a significantly higher efficiency. Using an 8x8 µm Impatt diode, an efficiency of 4.5% for a oscillation frequency of 104 GHz and an output power of 15 mW has been observed.

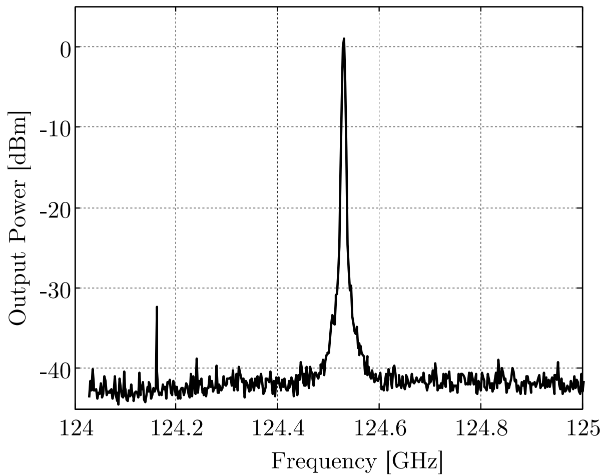

Fig. 14: Measured output spectrum of the Impatt oscillator for a biasing current of 22 mA.

The phase noise of the oscillator can be estimated from the measured power spectrum, shown in figure 15. With a receiver bandwidth of 1 MHz, the calculated phase noise is -95 dBc/ Hz in 10 MHz distance of the carrier.

VII. Conclusion

Monolithically integrated Impatt diodes on high resistivity silicon have been realized and characterized using S parameter measurement techniques. Based on the measured parameters, a millimeter wave oscillator has been designed, achieving an oscillation frequency of 124.5 GHz with an output power of 2 mW and an oscillation frequency of 104 GHz with and output power of 15 mW. Based on the S parameter measurements oscillator designs with enhanced efficiency are planned for the near future.

VIII. Acknowledgments

The authors would like to thank Michael Oehme and Klaus Matthies for manufacturing the presented devices.

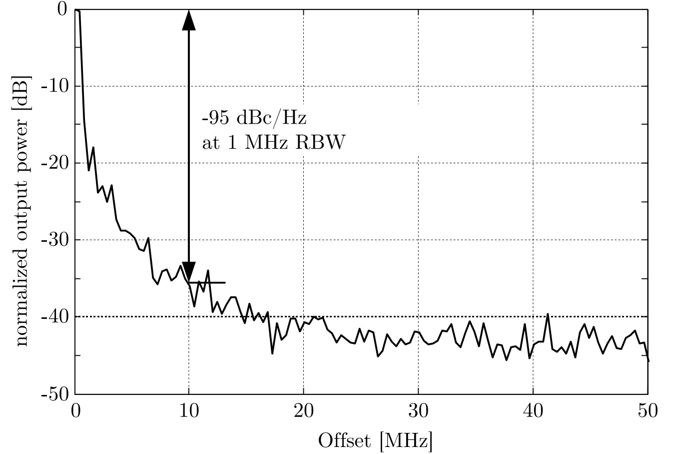

Fig. 15: Phase noise estimation from the measured output spectrum of the Impatt oscillator.

IX. References

[1] M. F. Tiemeijer and R. J. Havens, “An calibrated lumped-element de-embedding technique for on-wafer rf characterization of high-quality inductors and high-speed transistors,” vol. 50, pp. 822–829, 2003.

[2] E. Kasper, M. Oehme, K. Matthies, and J. Hasch *,to be published*.

[3] W. Read, “A proposed high-frequency negative resistance diode,” *Bell Syst. Tech. J.*, vol. 37, no. 401, p. any, 1958.

[4] K. Kurokawa, “Some basic characteristics of broadband negative resistance oscillator circuits,” *Bell Syst. Tech. J.*, vol. 48, no. 6, pp. 1937–1955, 1969.

[5] Farran Technology, *WHM-6 Harmonic Mixer*. http://www.farran.com, 2004.